

## Improvement of Helicopter Fuselage Modelling - Effects of subcomponents on the overall dynamic behavior

*J. Knebusch\**, *K. Soal\**, *R. Volkmar\**, *T. Meier\**, *D. Meier\**, *M. Altug†*, *R. Merce†*,  
*O. Dieterich†*, *M. Böswald\**

*\*DLR German Aerospace Center,  
Bunsenstrasse 10, 37073 Göttingen  
Germany*

*†Airbus Helicopter Germany,  
Industriestraße 4, 86609 Donauwörth  
Germany*

**Keywords:** Structural Dynamics, finite-element model, parameter-alteration, subcomponent, mode-tracking

**Abstract:** Like all aircraft, helicopters are designed to be as light as possible for the sake of low operational cost and minimum environmental footprint. Besides this lightweight construction, interaction between the rotor-blades and the air lead to strong oscillatory loads which are then introduced into the airframe of a helicopter. After significant improvement of aeromechanical modelling of helicopter rotors in the past decade, the loads can be simulated nowadays with reasonable accuracy. However, the ability to predict helicopter vibration using the simulation models of the fuselage is limited. The complexity of the helicopter fuselage structure poses challenges to both, experimental and numerical modal analysis. To achieve reasonably accurate forecast of the propagation of vibrations from the main rotor hub to different locations of interest an improvement of the simulation models is necessary. A shake test on a fully assembled helicopter is a too complex validation experiment for the targeted improvement of the simulation models. In order to address this inherent limitation, an extensive measurement campaign was conducted in the H135 helicopter production line in 2022. The vibration test team of the DLR-Institute of Aeroelasticity cooperated with vibration specialists from Airbus Helicopters Germany to plan and conduct ten modal tests on one helicopter successively built at different Assembly Stations. The modal tests took place during ongoing production operations. In conjunction finite-element models which represent the structural condition at each of the 10 production stations were created. The finite-element models of the respective helicopter components and subassemblies are used in this study to gain a better understanding of the influence of subcomponents on the overall dynamic behavior. In an experiment, a specific component can either be installed or not. Depending on stiffness and inertia properties of the components, the changes in dynamic behavior can be considerable and changes in mode shapes and eigenfrequencies are hard to track in experimental data. In numerical simulation, however, a smooth “blending in” of components is possible enabling the tracking of changes of modal parameters when installing specific components to a helicopter subassembly. This new approach to finite-element model updating is presented here. In this, stiffness and mass values are gradually increased (from 5% to 150% of the nominal value in small steps of 1%) for entire components that get mounted at the respective Assembly Station. A numerical modal analysis is performed after each alteration. The alterations and their influence on eigenfrequency and mode shapes are tracked over the different stations. This approach seems promising for the use on Helicopters (and complex structures in general) and could also be used

for the development of new prototypes. The approach presented here can be considered as a pre-conditioning step of the corresponding finite-element models, to be applied in case of deviations between test and analysis being too large to conduct sensitivity-based finite-element model updating as explained in [1].

## 1 INTRODUCTION

On the one hand, helicopters, like all aircraft, require lightweight construction in order to minimize the environmental impact while maximizing performance, range and cost efficiency. On the other hand, the interaction between the air and the rotor leads to large oscillatory forces which are then introduced into the light-weight airframe via the main rotor hub. While the accuracy of the simulation of these aeromechanical loads has improved significantly over the past 10 years, predicting vibration propagation in the airframe remains challenging.

To further improve the accuracy of Helicopter airframe simulation results, a combined numerical and experimental approach was developed by Airbus Helicopters and DLR. An extensive experimental modal test campaign was conducted during different assembly stages on a H135 in the production line. The DLR-Institute of Aeroelasticity collaborated with vibration specialists from Airbus Helicopters to perform ten modal tests during ongoing production operations, aiming to improve simulation models. Airbus Helicopters created finite-element models that match the different structural states in which the helicopter was tested. An overview of the Helicopter in the different stages of production in which it was tested is shown Figure 1.

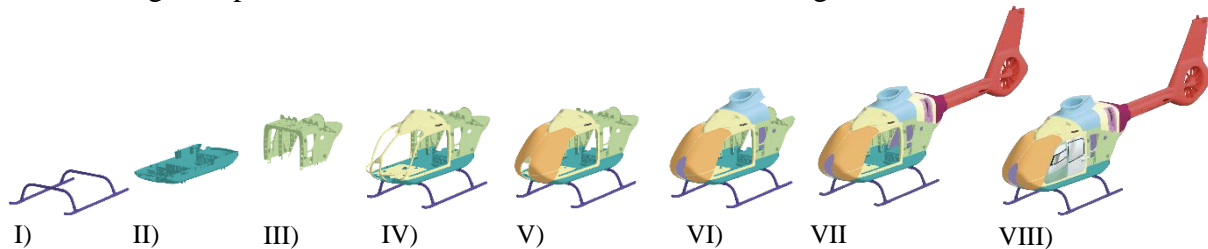


Figure 1: Assembly stages in which experimental modal tests were conducted

Since mode shapes and eigenfrequencies can change significantly by the installation of one sub-component, correlation of modal results from one production state to the next production state can be challenging. Quite often, only a few mode shapes can be correlated, which is a poor database to understand the effect of installing a subcomponent. This publication shows an approach to circumvent this limitation. Using numerical simulations certain components get blended in, by a gradual increase of their mass- and stiffness property values starting from 5% of their nominal values in steps of 1% up to 150%.

The changes of mode shapes and eigenfrequencies from 1% change in mass and stiffness are thus significantly smaller than for the experimental counterpart, where the respective subcomponent can only get mounted completely (i.e. 0% or 100%). This simplifies the tracking of the modes of vibration (in short: “modes”) from one parameter alteration to the next. Parameter studies in general are a well-established tool and mode-tracking is a known technique e.g. from flight-vibration testing ([1],[3]). The combined use of both techniques on an industrial-scale finite-element model has, to the knowledge of the authors, not been published before. A laboratory structure has been investigated with a similar approach in [4], but unlike our study, it does not show the effect of parameter changes on entire components. In the following, an overview of the finite-element model is given, the mode-tracking is explained and the key aspects of the results are shown, before a conclusion is drawn and an outlook is given.

## 2 FINITE-ELEMENT MODEL

The baseline finite-element models used in this study are of an industrial scale and use approximately 150.000 to 250.000 elements. This relatively coarse meshing originates from the 1990ies when the helicopter type was developed. Nonetheless, the model is suitable for numerical modal analysis. The models are investigated using free-free boundary conditions. Subcomponents, that are highlighted with different colors and named in Figure 2, are altered in this study. This alteration is performed for entire subcomponents (Center Fuselage Section (CFS), Landing Gear (LG), Bottom Shell (BS), Window (WND), Main Gear Box (MGB)) in terms of mass and stiffness. Mass and stiffness are altered from 5% of their nominal value to 150% of their nominal value in 1% steps. For each subcomponent the parameters (mass and stiffness) are altered separately as well as simultaneously in three separate investigations per subcomponent. After each alteration, a numerical modal analysis of the model is performed (Nastran SOL103). The components are altered at the respective Assembly Station at which they get mounted (as shown in Figure 2 a) and b)) and at the Assembly Station at which the Helicopter is almost fully assembled (Figure 2 c)) and ready for a helicopter Shake Test (as described in [5],[6]). In the following, a parameter alteration in steps of 1% from 5% to 150% on one component at a specific Assembly Station is termed a “group of alterations”. The parameter values are increased beyond their nominal value of 100% to see effects of over- as-well as underestimations of mass- and stiffness properties.

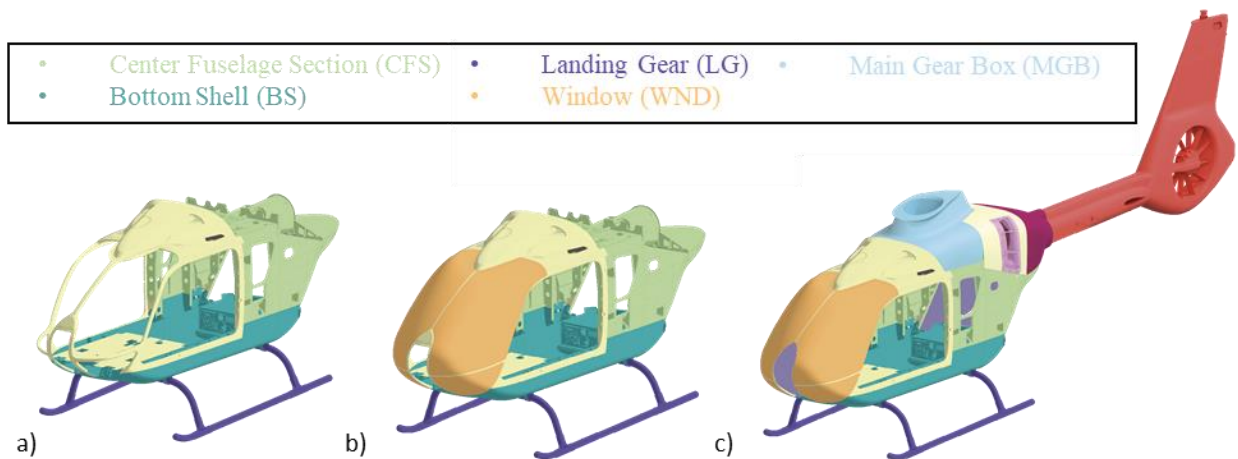


Figure 2: FE-models of assemblies at different stages: a) Assembly Station IV b) Assembly Station V c) Assembly Station VIII

## 3 MODE TRACKING

In order to judge the influence of parameter alterations, the modes of a group of alterations, have to be correlated with each other. Figure 3 sketches this process. Each numerical modal analysis (Nastran SOL103) after a parameter alteration delivers a mode set (consisting of mode shapes and eigenfrequencies) for every mode of vibration within the frequency range of interest. The eigenfrequencies of 16 mode sets are exemplarily plotted as squares over a parameter variation in Figure 3 (left). The mode sets are highlighted using green and red rectangles.

The results from subsequent mode sets now have to be grouped into mode families (as detailed in [1]). This grouping is achieved based on a suitable similarity criterion.

One way of assessing similarity between modes of vibration is the Modal Assurance Criterion (MAC). The criterion (1) is defined as the normalized dot product between two modes  $\psi_p$  and  $\psi_q$ , where  $T$  indicates a transposition of the respective mode shape and  $*$  indicates the complex conjugate of a mode shape [7]

$$\text{MAC}(\psi_p, \psi_q) = \frac{|(\psi_p^T \cdot \psi_q)|^2}{(\psi_p^T \cdot \psi_p^*)(\psi_q^T \cdot \psi_q^*)} \quad (1)$$

For two collinear modes, this value is 100% and for two orthogonal modes, this value is 0%. If the MAC criterion is applied to all modes of the modal matrix, this results in a MAC matrix. High MAC values indicate mode shape similarity while low values indicate dissimilarity. If mode shapes  $p$  and  $q$  are from the same mode shape matrix, the calculated values are called AUTOMAC-values [8].

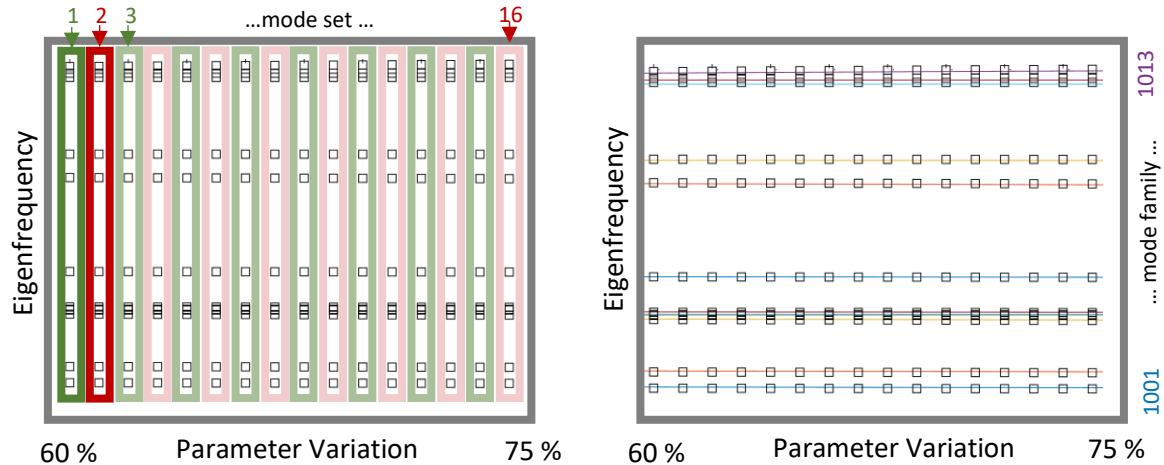


Figure 3: Mode tracking – modes of vibration of result sets from subsequent numerical modal analysis (left) have to be related to each other and combined into mode families (right)

The MAC criterion is calculated for two subsequent result sets. These result sets are created using finite-element models which differ by 1% in terms of mass and/or stiffness of one subcomponent. The pairs of mode shapes which have the highest MAC-value of all possible pairs (while exceeding a minimum threshold MAC-value of 95%) are grouped into the same mode family. Unlike experimental results, these simulated modal results are not contaminated by distorting influences (e.g. noise, identification inaccuracy, etc.). Considering that the highest MAC values in the example in Figure 5 (left) are on the main diagonal, the order of the modes of vibration in the given example does not change. Since this is also the case for the subsequent pairs of result sets (e.g. the MAC values between mode set 2 and mode set 3) the horizontal lines of the 12 mode families do not cross.

Since the computational requirements in terms of storage and memory of using results from all degrees of freedom and every result set are considerable (circa 500 megabytes per result file and thus 75 gigabytes per group of alterations) the results were reduced to selected output degrees of freedom. The order of the finite-element models remains unchanged, only the number of output degrees of freedom is reduced. The selected degrees of freedom are intended to capture global mode shapes and shown using red, green and blue arrows for the three spatial directions (x,y,z) in Figure 4 b). The reduction of degrees of freedom leads to a slightly poorer observability but reduces the computational requirements roughly by a factor of 10. Thus, it allows the computation on a standard multi-core PC with fair amount of RAM, rather than a high-performance computer cluster. The selected positions were largely used as sensor positions in the accompanying experimental test

campaign (described in [10]) and therein served well for capturing the global mode shapes. The reduced set of degrees of freedom is used consistently for all mode tracking conducted in this study.

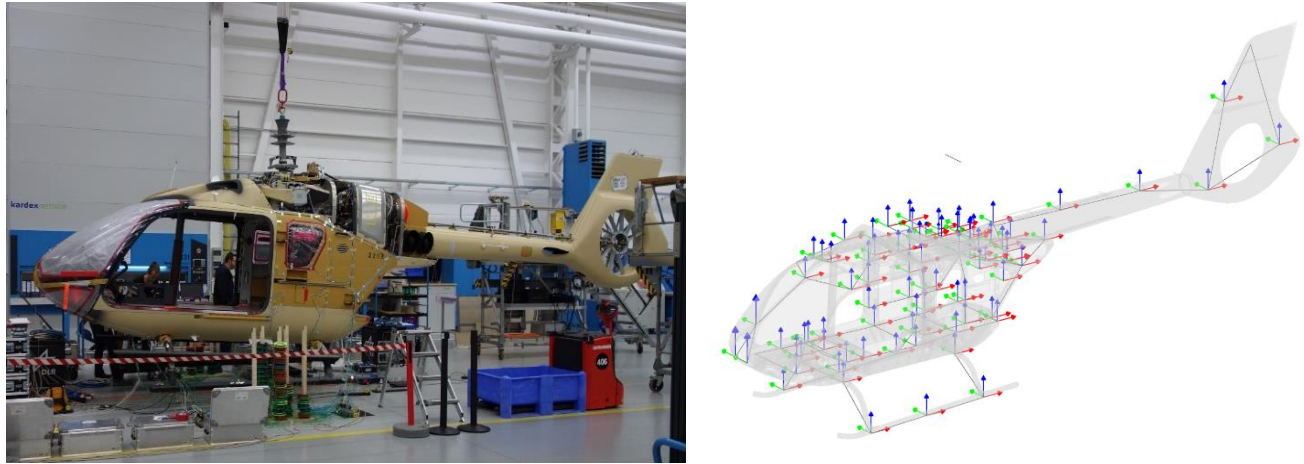


Figure 4: a) Tested helicopter b) selected degrees of freedom on finite-element grid

This requires, that the degree of freedom has to be part of a substructure which is included in the respective finite-element model. For example, the degrees of freedom on the Tailboom (Figure 2 c) are not included in the finite-element model of Assembly Station IV.

When the results are reduced to the selected degrees of freedom and the MAC-matrix between result set 1 and result set 2 is calculated (Figure 5 (right)), some off-diagonal values, especially for the modes #11-#13, are higher than in case of the full set of output degrees of freedom (Figure 5 (left)). It ought to be noted, that these modes of vibration for which the off-diagonal MAC-values are high, are local modes rather than global modes. In addition, high MAC-values on off-diagonal elements can occur especially for systems with concentrated masses instead of uniformly distributed mass. Due to the significant masses of discrete systems like the main gear, off-diagonal terms were expected to appear.

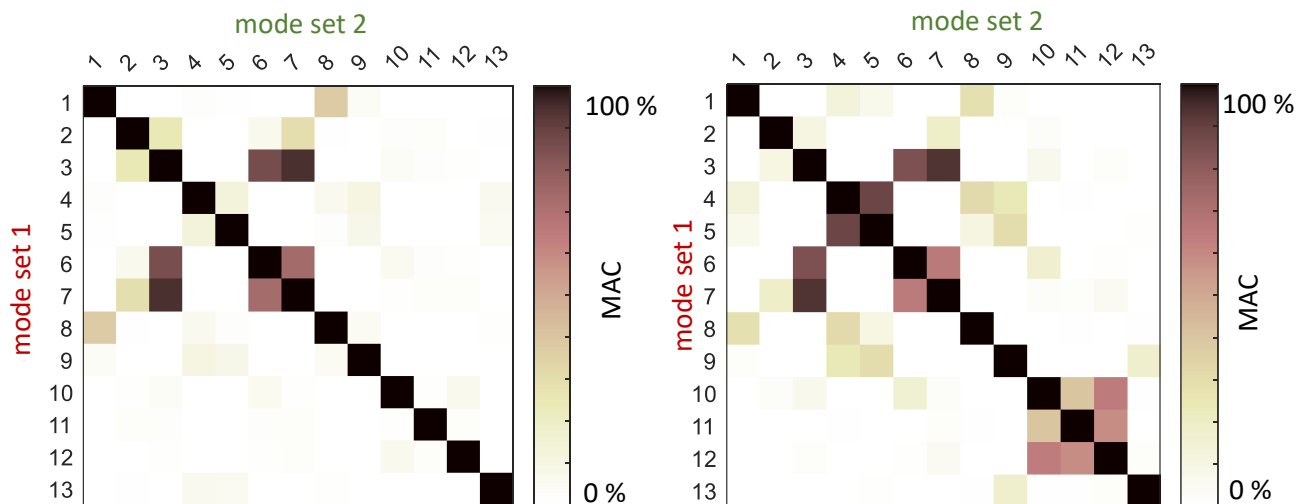


Figure 5: MAC-criterion for all degrees of freedom (left) and reduced to selected degrees of freedom (right)

The previous paragraphs described the basic approach to tracking modes of vibration. While this tracking approach is sufficient for modes which do not change significantly with parameter alterations, it has to be slightly adapted in order to be able to deal with modes that show high changes over the parameter alteration. An example of this is given in Figure 6. Here the effect of mass alterations of the entire Bottom Shell (BS) in the structural state of Assembly Station IV are shown. On the left side one can see eigenfrequencies of the tracked mode families over the parameter alteration colored by their mode family number (Figure 6 a)). It is important to note, that not only the eigenfrequencies but also the mode shapes change over the parameter alterations. The center plot shows the same lines as Figure 6 a), but they are colored by the MAC value between subsequent members of each mode family (Figure 3 b)). Since the minimum requirement for mode shape pairs to be considered is 95%, all lines in this center plot are black. The lines in the plot on the right-hand side are colored by the average off-diagonal AUTOMAC-value of the respective mode family (Figure 6 c)). The red- and orange color therefore show, that while subsequent modes of a mode family have a high similarity, not all modes within those mode families have a high similarity. This is detailed in Figure 7 for one selected mode family. That mode family has an orange line and is indicated by the blue arrow Figure 6 a). As per the above described process, the modes were tracked into this mode family by starting with mode set 1 and mode set 2, in other words the results of the simulations for which the mass of the Bottom Shell was lowered to 5% and 6% of its nominal value. The mode tracking then proceeded with the subsequent mode sets, up to a parameter value of 150%. From the AUTOMAC-matrix in Figure 7 a) one can, see, that the modes which are grouped into this mode family actually belong to three different sub-families. The two largest of these three sub-families transition from one to the other at a mass-alteration value of approximately 90 %. There is no sharp change from one sub-family to the next, but a transition area (highlighted with a red rectangle). As one can see, the corresponding mode shape is rather constant from 5% to 86%. Then a significant change in the mode shape vector occurs from 86% to 94%. Afterwards the mode shape is again not very sensitive to changes in the parameter, until another change takes place in the vicinity of 135%. There is obviously no linear relation between change of mode shape vector and change of structural parameter.

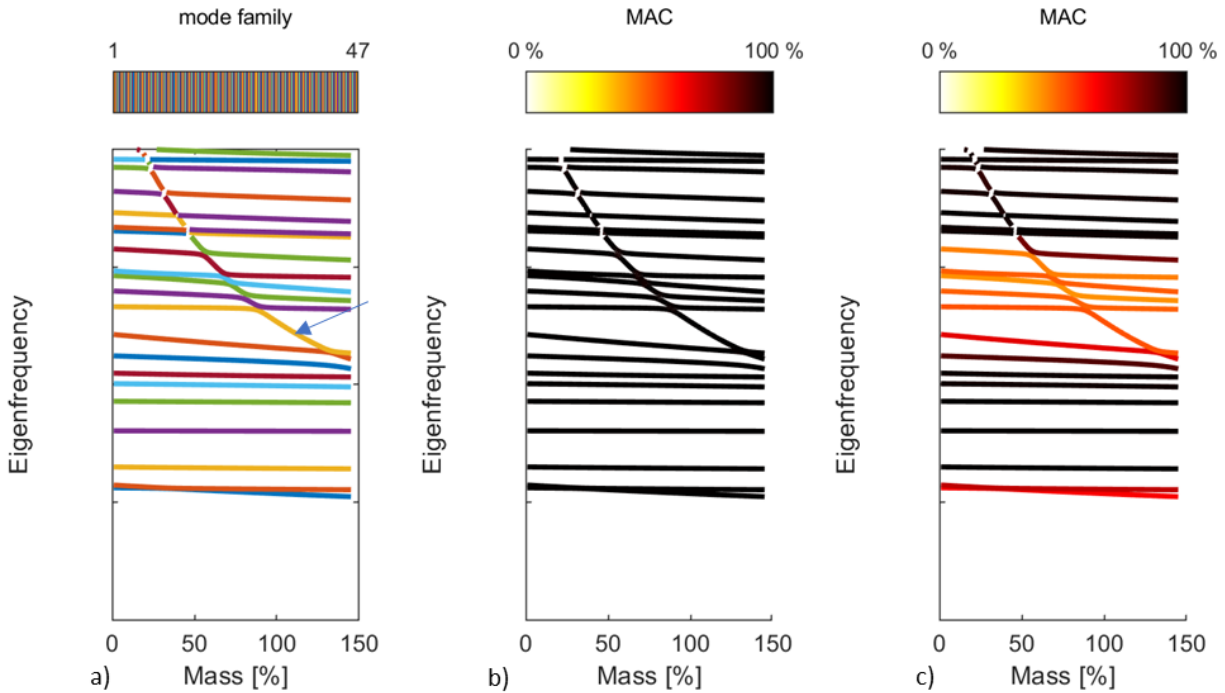


Figure 6: Tracked mode shapes, lines colored by: a) family number, b) MAC value of subsequent modes within a family, c) average off-diagonal MAC-value within a family || blue arrow in a) points to mode family detailed in Figure 6

The AUTOMAC-matrix in Figure 7 b) is zoomed into this “transition region” and shows, that while the MAC-values between modes which are far away from each other are low, nearby MAC-values in this transition region are high. Since “only” the results of neighboring alterations are compared and related to each other, the transition region between the sub-family leads to the them being connected and therefore categorized as one mode family.

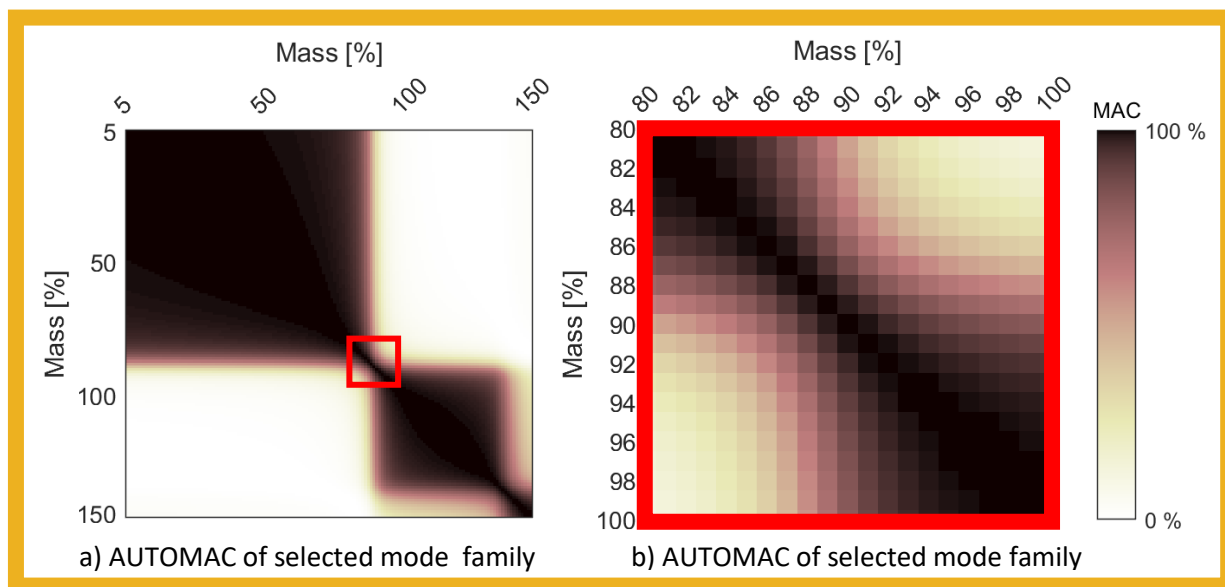


Figure 7: AUTOMAC matrix for selected mode family || a) full matrix, b) zoom into transition region

Figure 8 exemplarily shows mode shapes which represent modes from the three respective sub-families. Since the mode shapes within each sub-family are very similar, as can be seen from the

dark regions in the AUTOMAC-Matrix (Figure 7 a)), it is sufficient to look at one mode shape per sub-family as opposed to all of them.

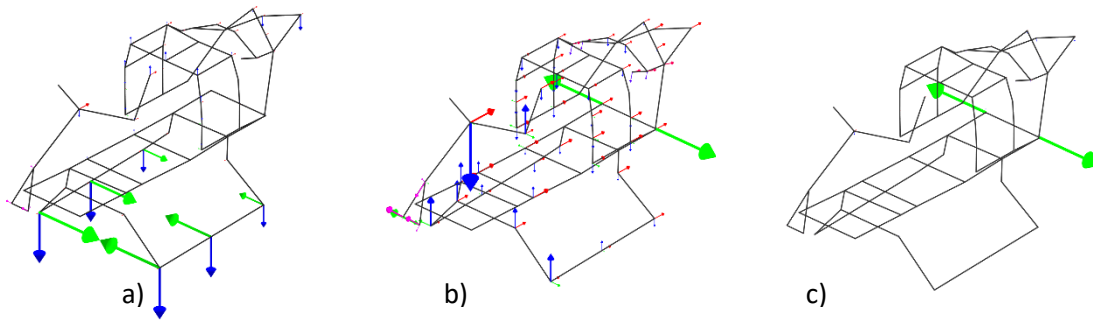


Figure 8: Exemplary mode shape plot for sub-families within selected mode family: a) “5%-mass” b) 125%-mass c) 150%-mass

In conclusion, the mode shapes on the left limit of the diagram are not the same ones on the right limit of the diagram. Not only eigenfrequencies change, but also eigenvectors.

In order to circumvent this shortcoming, the tracking-criterion is marginally adapted. The MAC value is now calculated between one mode set and the mean of 10 previous mode sets. The average over 10 mode sets is calculated by scaling the mode shapes to “largest component 1” and orienting the mode shapes in the same direction by multiplying them with the appropriate sign. This averaging procedure is used and described in [9]. In utilizing this criterion in the mode-tracking, the previously described sub-families are split into separate mode families. This is because the mode shapes at the edges of the sub-families are not compared to their direct neighbors in the transition region, but to the average of the last 10 mode shapes which also reach outside the transition region. The blue arrow in Figure 9 a) shows, that the mode family is now split apart. The thereby created families are colored in green and yellow. The colorbar in the top of Figure 9 a) also indicates that this is not the only split of mode families. The same alteration group is now categorized into 86 mode families instead of the previously shown 47 mode families (Figure 6 a). This maintains the previously described high-MAC value of subsequent modes within a mode family and leads to significantly higher average MAC-values within each mode family (Figure 9 b) c)).



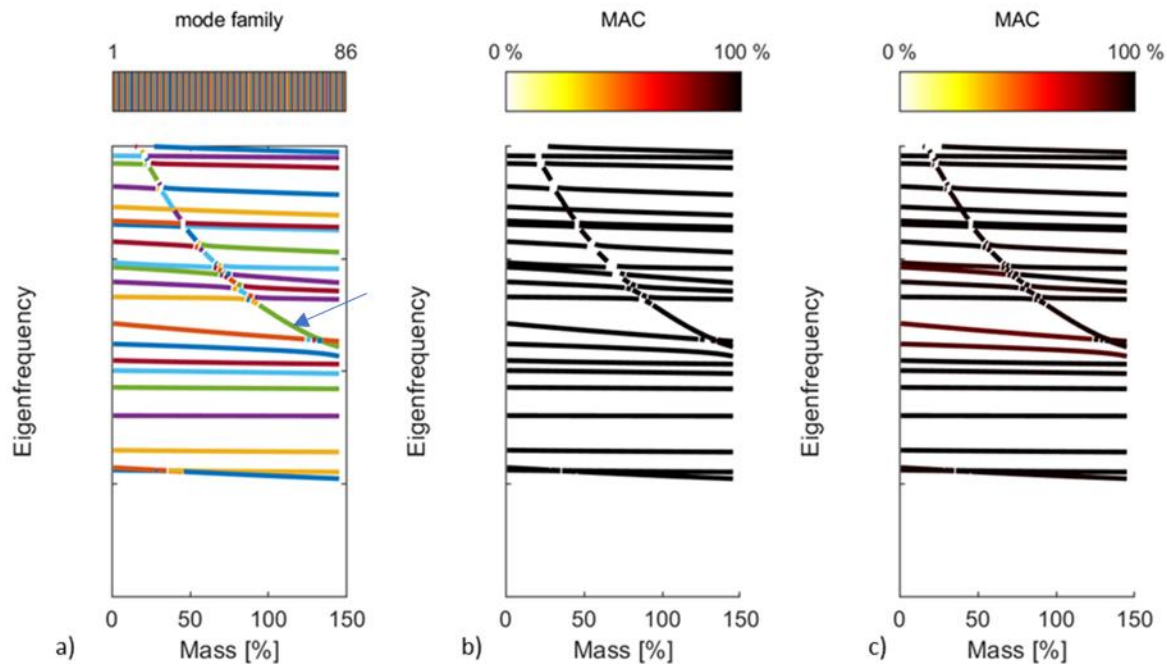


Figure 9: Tracked mode shapes using averaging, lines colored by: a) family number, b) MAC value of subsequent modes within a family, c) average off-diagonal MAC-value within a family || blue arrow in a) points to second sub-family detailed in Figure 6

In order to judge if a parameter change is relevant it is helpful to focus on certain modes. Several aspects determine, if a given mode is especially important. Some modes are relevant because their eigenfrequency is in a specific frequency band (e.g. multiples of the reference rotation frequency of the main rotor) and others are known to have undesired effects. Besides this, there is another group of modes which is particularly relevant for the understanding of the overall dynamic behavior. These are global modes. Global modes as opposed to local modes are modes for which a significant part of the structure participates (i.e. vibrates). There is, to the knowledge of the authors, no established objective criterion to assess whether a simulated mode is a global or a local mode shape. The modes are therefore ranked in the following four steps in order to judge if they are “global” or “local” modes.

1. The mode shapes vectors are scaled, such that their largest entry is one.
2. The absolute entries of the mode shape vectors are summed.
3. These sums are normalized by the maximum of all calculated sums.
4. These values are sorted in descending order (i.e. from global to local) and herein called Global Mode Indicator (GMI).

Figure 10 exemplarily shows the sorted GMI for Assembly Station IV for all modes in the frequency range of interest. The top of Figure 10 furthermore gives examples for high, medium and low GMIs by showing the respective mode shapes for a GMI of 100%, 27% and 6%. Especially when comparing the mode on the left with the mode on the right, it becomes clear, that the calculated value is in this case indicative of a global or a local behavior.

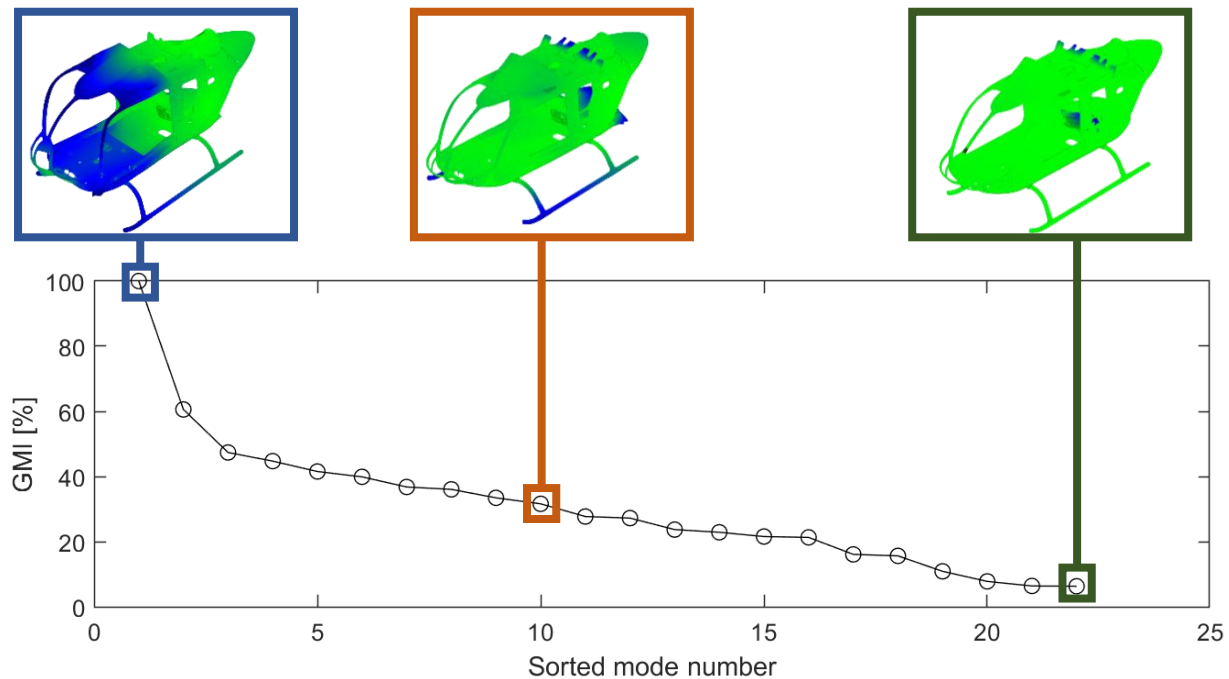


Figure 10: Mode shapes of Assembly Station IV, ordered by their Global Mode Indicator (GMI)

## 4 RESULTS

In the following section an overview of the results is given. The mode-tracking which was explained in the previous section is now used to show the effects of parameter changes of entire components on the overall dynamic behavior. When changes on multiple components are overlaid in one plot, the colors of the lines are the same as for the respective component in

Figure 2. The particularly important global mode families are shown in dark lines, while other families are not investigated further and shown in light lines for completeness. Global modes are highlighted with a red pentagram at the nominal parameter value of 100%.

Figure 12 gives an overview of the effects of combined mass and stiffness changes on the eigenfrequencies of ten global modes at Assembly Station VIII. It can be seen, that the effects of parameter changes of different subcomponents on the overall dynamic behavior and the eigenfrequencies of the selected modes in particular varies significantly. For example, the first global mode (Figure 11 a)) is mainly affected by parameter changes on the Center Fuselage Section. For the first four global modes (Figure 11 a)-d)), alterations on the Landing Gear and the Windows do not lead to large changes in eigenfrequencies. The corresponding orange and purple lines are therefore almost horizontal. When comparing the effects of “blending in” the Landing Gear for the 8<sup>th</sup> and the 9<sup>th</sup> global mode, it becomes obvious, that it has a stiffening effect for the former (Figure 11 h)) and a mass-related effect for the later (Figure 11 i)). Due to the considerable slope of the respective purple lines (i.e. the change in eigenfrequencies) this is particularly important.

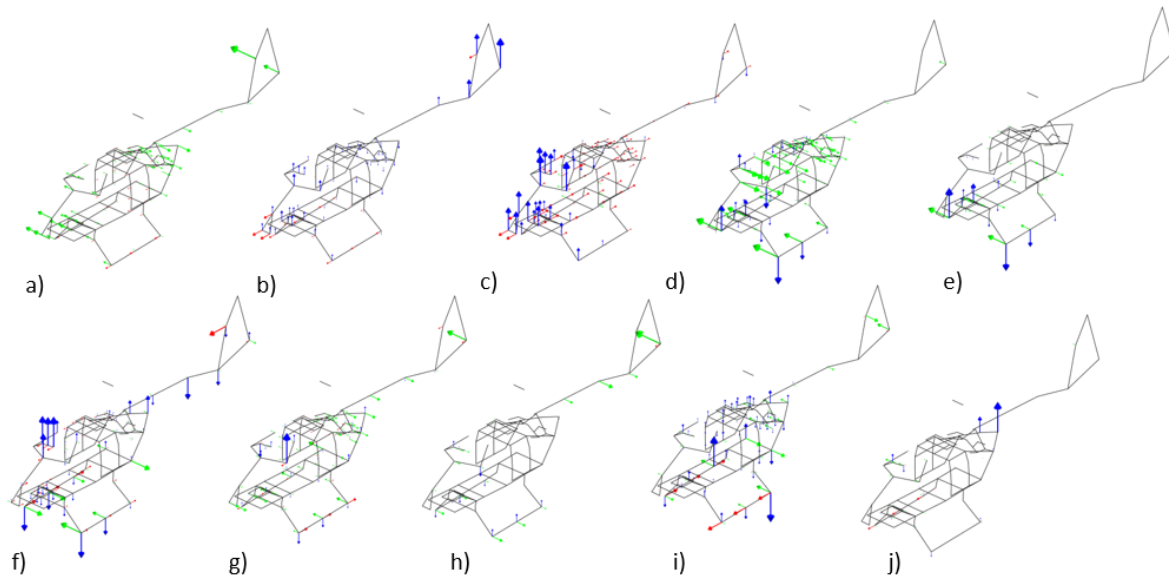


Figure 11: First 10 global mode shapes at Assembly Station VIII ordered by ascending frequency (a - j))

Table 1 gives the linearized slope of the respective dark colored lines around the nominal parameter values. To calculate this, the changes in eigenfrequency  $\Delta f$  between the upper (110%) and the lower bound (90%), are divided by the parameter-changes  $\Delta p$  between the bounds. The upper- and the lower bounds are shown by the dashed vertical lines in Figure 12. This quantifies the previously described visual impression of how relevant changes of parameters on certain components are and can help in subsequent computational model-updating studies.

Table 1: Linearized slope ( $\Delta f / \Delta p$ ) around nominal parameter value (90 % - 110 %) on different subcomponents for global modes (a-j))

	a)	b)	c)	d)	e)	f)	g)	h)	i)	j)
<b>CFS</b>	0,42	1,1	0,74	1,16	1,97	1,8	1,5	1,53	2,61	1,92
<b>BS</b>	-0,03	0,26	0,8	0,73	1,79	1,28	2,76	0,45	2,78	1,58
<b>LG</b>	-0,11	-0,15	-0,05	-0,46	-2,07	-0,70	-0,53	0,25	-2,18	-0,46
<b>WND</b>	0,00	0,02	0,05	0,03	0,42	0,41	0,27	0,20	0,39	1,26

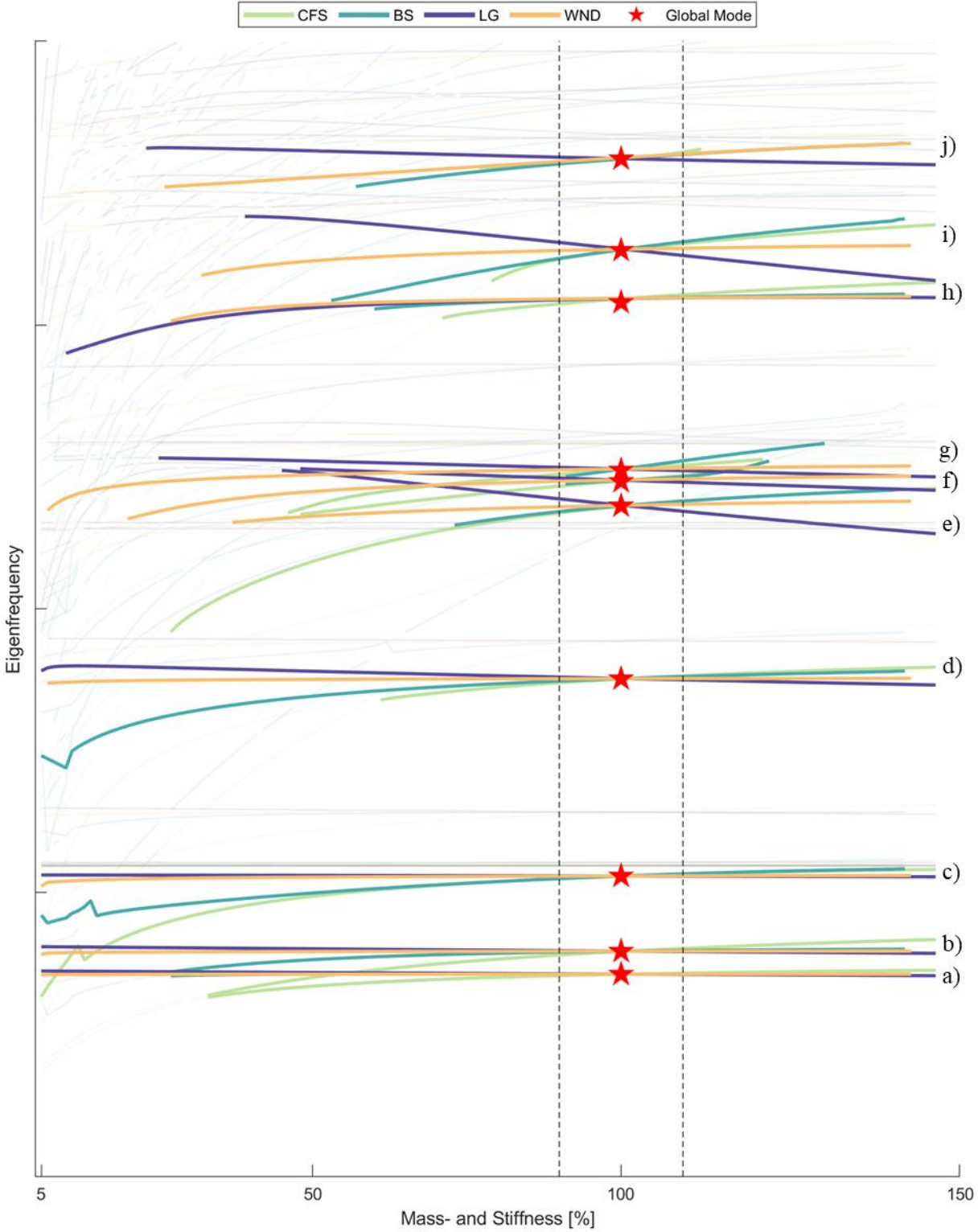


Figure 12: Effects of combined mass- and stiffness alterations on different subcomponents

Another key finding is, that for almost all altered components, the change of the dynamic behavior due to mass alteration is significantly smaller than due to stiffness alteration. Consequently, when altering mass and stiffness simultaneously with the same percentage, the effects of the stiffness

alterations is prevalent. One important aspect that partly leads to this, is that only the mass of the primary structure and not the mass of secondary structures (i.e. concentrated masses, apart from MGB) is altered. Furthermore, since helicopters are lightweight-constructions, the mass-to-stiffness ratio is low for most subcomponents. In light of this, the respective equation of motion is influenced more by changes in the stiffness-matrix than by changes in the mass-matrix. An example of this is given for five global mode families in Figure 13. One can see, that the orange- and the yellow lines are almost congruent, whereas the blue line is almost straight. Figure 13 also shows, that the effect of parameter alterations below  $\pm 20\%$  of its nominal value (i.e. between 80% and 120%) on the eigenfrequencies of the five selected global modes is small (below 5%).

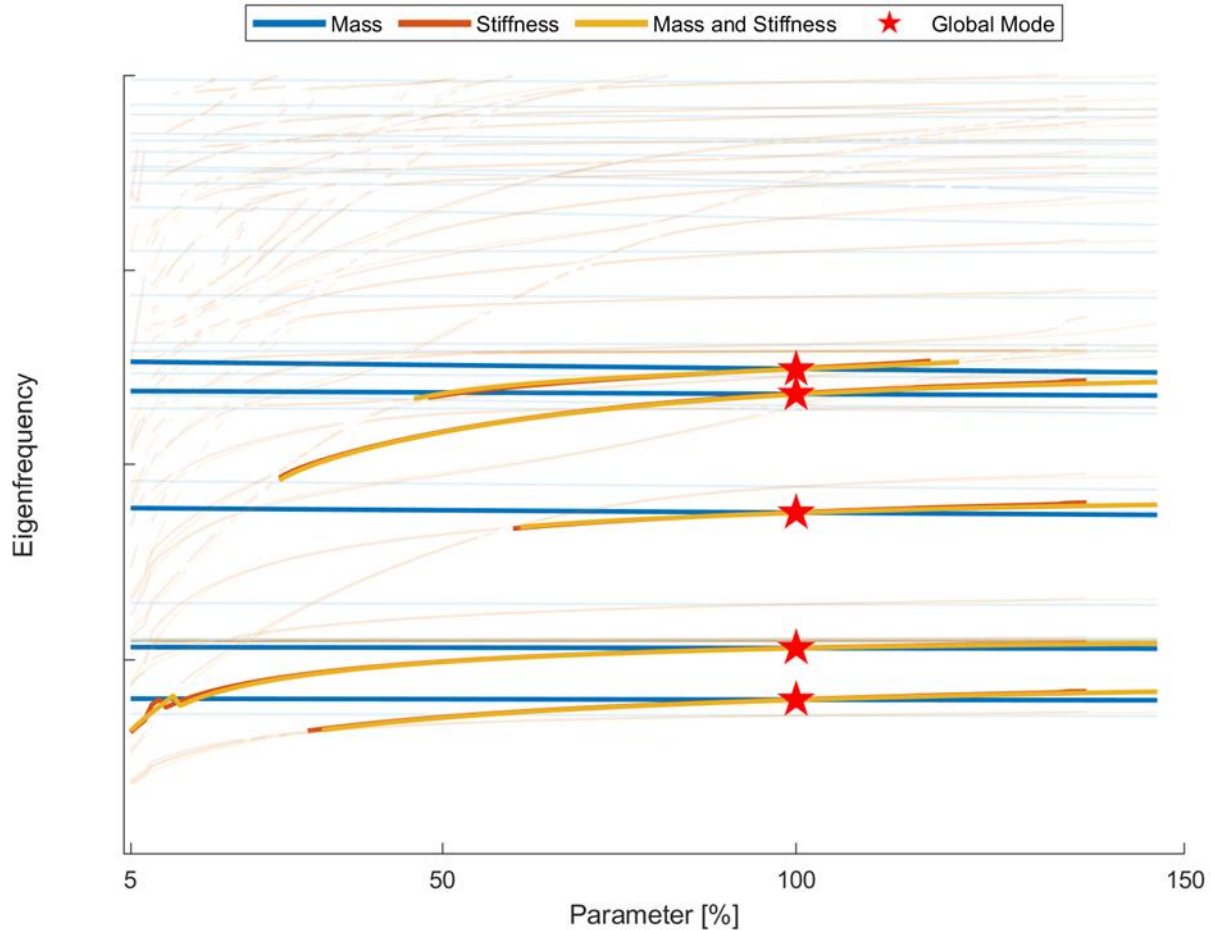


Figure 13: Altered Parameters on Center Fuselage Section at Assembly Station VIII

The windows are an exception to this general observation. Since the windows are made out of acrylic glass, the stiffness of the windows compared to their weight is relatively low. Figure 14 shows, the effects of mass-, stiffness- and combined mass- and stiffness changes of the windows on the overall dynamic behaviour at Assembly Station V. It becomes clear, that while combined alterations lead to small changes, separate alterations of mass as well as stiffness lead to significant changes. The effects of combined alterations mostly cancel each other out. This is noteworthy, when considering the effects of erroneous nominal stiffness- and mass matrices. Mass- and stiffness properties can be deviating from their true value by the same factor, for example because of wrong thickness estimations. Erroneous nominal material properties can also occur, if the properties determined on a coupon level do not match those of a substructure. In that case, mass- and stiffness deviations are not directly related.

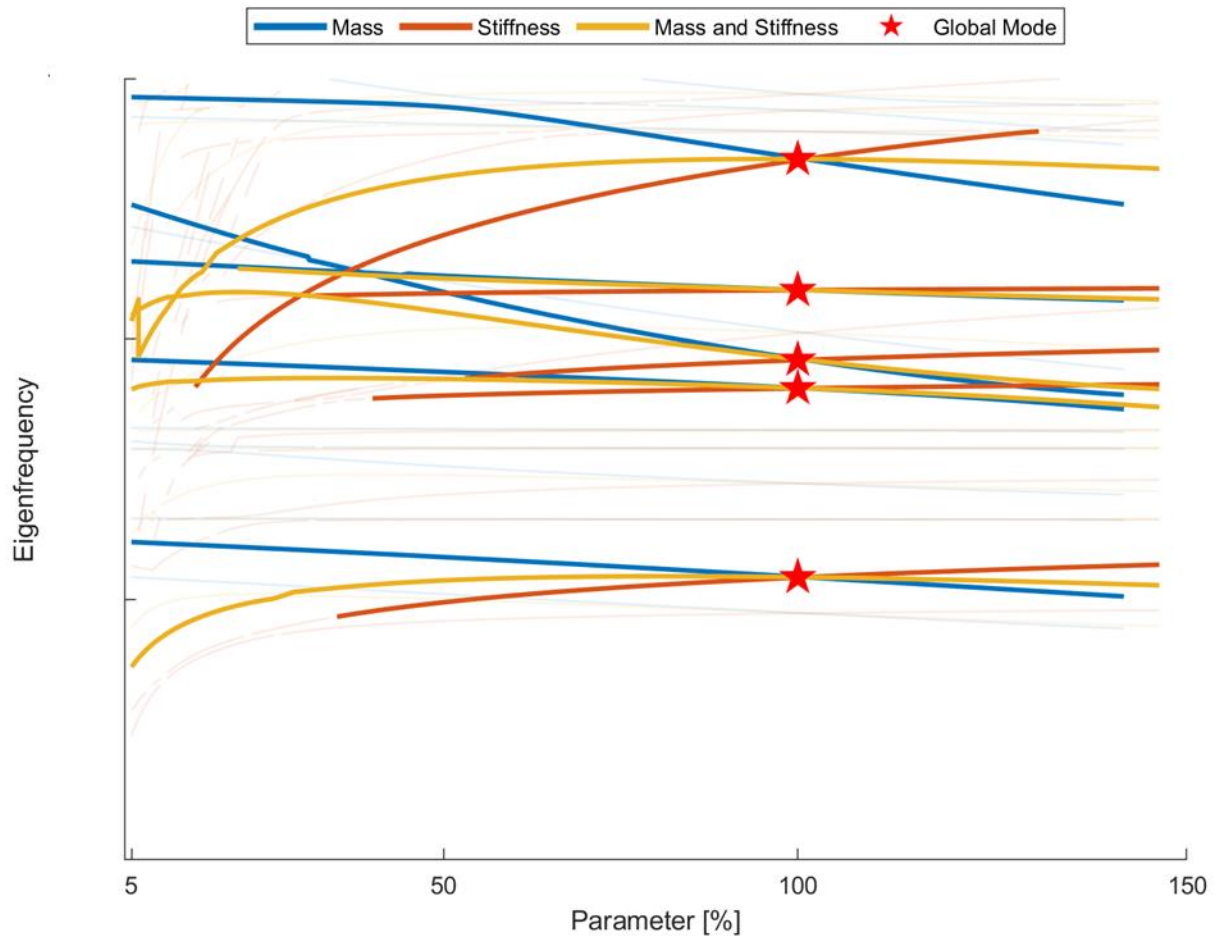


Figure 14: Altered Parameters on windows at Assembly Station V

The previous paragraphs focused on the effects of parameter changes of subcomponents which are considered in the finite-element model as fully meshed parts. In the following, the effects of parameter changes on the main gear box, which is represented by a concentrated mass element, is described. In spite of its comparatively large absolute mass, varying the mass of the gear box effects the eigenfrequencies only slightly. However, the average MAC within each mode family, which is plotted in Figure 15, shows that some mode shapes are changed significantly by this alteration. This mainly occurs in the higher frequency regime and on mode shapes which mainly exhibit a distinct local behavior.

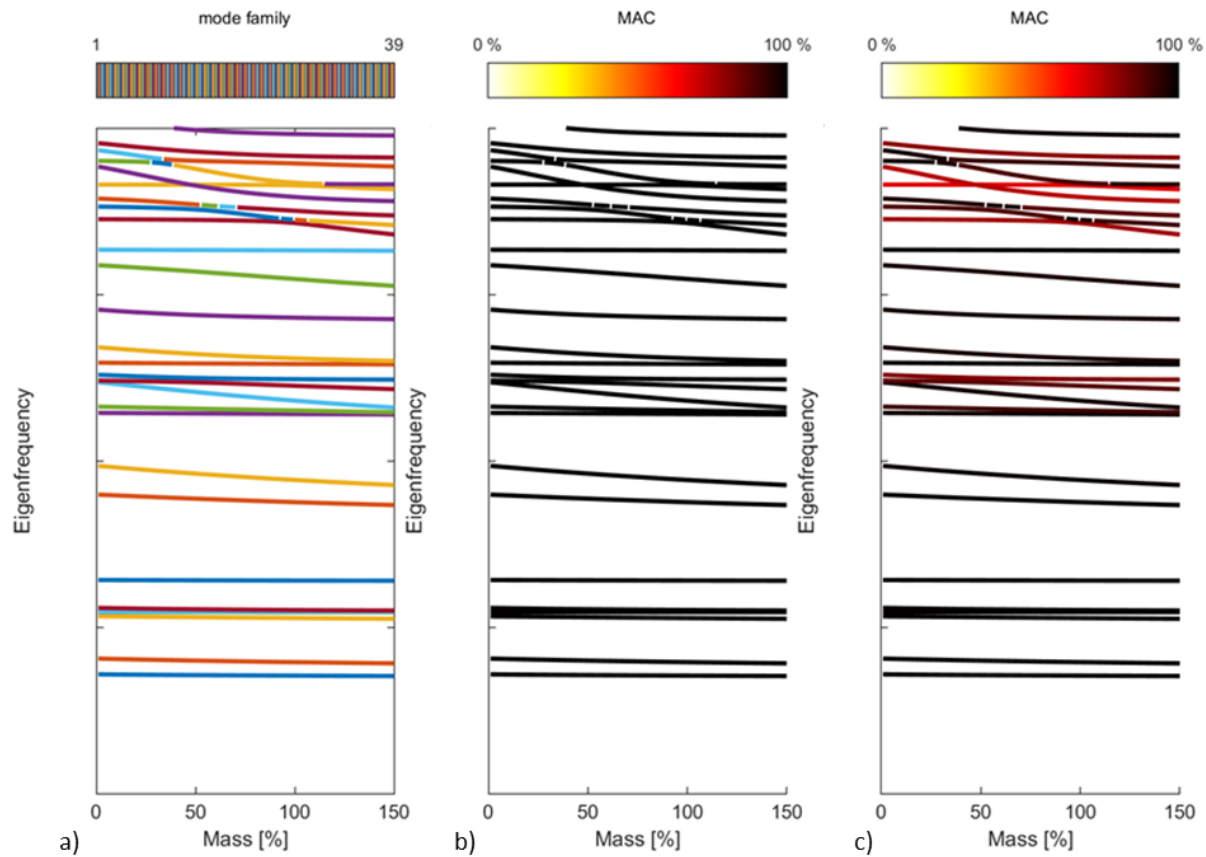


Figure 15: Altered mass of main gear box at Assembly Station VIII, lines colored by: a) family number, b) MAC value of subsequent modes within a family, c) average off-diagonal MAC-value within a family

With the described approach, the sensitivity of modes to parameter changes of entire subcomponents on a wide range of parameters can be calculated and easily assessed. Unlike in classical model updating, where the sensitivities are calculated only in the vicinity of the nominal parameter values [1], this allows to judge how subcomponents affect the dynamic behavior at large. It is not considered a replacement to classical model-updating but rather a reasonable preconditioning step.

## 5 CONCLUSION AND OUTLOOK

Using the presented combination of parameter alterations on entire subcomponents with a suitable mode tracking algorithm enables the understanding of the effect of parameter changes on the overall dynamic behavior. It is described, that the established MAC-based mode-tracking cannot be applied as is, but has to be extended by mode shape averaging over past parameter variations for the present case. Even though this extension works well, it is considered a pragmatic solution rather than the optimal approach to tracking simulated modes. Eigenvector tracking in general is an active field of research. Various algorithms for tracking eigenvectors of parameter varied systems exist (e.g. as presented in [12], [13] and [14]) and ought to be assessed for this particular application.

Using the MAC-based mode shape averaged tracking approach, the effect of parameter alterations on global modes are detailed. Changes which have a particularly strong effect are highlighted and put into perspective. It is noteworthy, that not only changes of eigenfrequencies, but also of mode

shapes are recognized and shown. Given the improved understanding of the effects of mass- and stiffness changes of subcomponents on the overall dynamic behavior, the approach will be utilized and extended in future works.

## Acknowledgement

Supported by:



on the basis of a decision  
by the German Bundestag

The eVolve project is supported by the Ministry of Economic Affairs and Climate Action within the German national civil aviation research programme (LuFo VI-1, FKZ 20A1902E).

## REFERENCES

- [1] Mottershead, J. E., Link, M., & Friswell, M. I. (2011). The sensitivity method in finite element model updating: A tutorial. *Mechanical systems and signal processing*, 25(7), 2275-2296.
- [2] Jeličić, G. (2022). System Identification of Parameter-Varying Aeroelastic Systems using Real-Time Operational Modal Analysis DLR-Forschungsbericht. DLR-FB-2022-6. Dissertation. Syddansk Universitet (SDU). 343 S.
- [3] Böswald, M., Schwochow, J., Jelcic, G., & Govers, Y. (2017, June). Recent developments in operational modal analysis for ground and flight vibration testing. In International Forum on Aeroelasticity and Structural Dynamics IFASD.
- [4] Towner, R., & Band, J. (2012, April). An analysis technique/automated tool for comparing and tracking analysis modes of different finite element models. In 53rd AIAA/ASME/ASCE/AHS/ASC Structures, Structural Dynamics and Materials Conference 20th AIAA/ASME/AHS Adaptive Structures Conference 14th AIAA (p. 1987).
- [5] Ciavarella, Christopher und Priems, Martijn und Govers, Yves und Böswald, Marc (2018) [An extensive helicopter Ground Vibration Test: from pretest analysis to the study of nonlinearities.](#) In: 44th European Rotorcraft Forum 2018, ERF 2018. ERF 2018 - 44th European Rotorcraft Forum, 2018-09-18 - 2018-09-21, Delft, Netherlands.
- [6] Sinske et. al. (2024) Research Shake Test on an Airbus Helicopters technology Demonstrator (2024), to be published in IFASD 2024, International Forum on Aeroelasticity and Structural Dynamics, The Hague, The Netherlands
- [7] Allemang, R. J. (2003). The modal assurance criterion—twenty years of use and abuse. *Sound and vibration*, 37(8), 14-23.
- [8] Ewins, D. J. (2000). Model validation: Correlation for updating. *Sadhana*, 25(3), 221-234



- [9] Govers, Y., & Link, M. (2010). Stochastic model updating of an aircraft like structure by parameter covariance matrix adjustment. In Proc. of the International Conference on Noise and Vibration Engineering, ISMA.
- [10] Knebusch J., Soal K., Altug M., Dieterich O. and Böswald M., (2024). Subcomponent modal tests in the H135-production line to further improve finite-element model updating, to be published in: 50th European Rotorcraft Forum 2024, Marseille, France
- [11] Ewins, D. J. (2009). Modal testing: theory, practice and application. John Wiley & Sons.
- [12] Pradovera, D., & Borghi, A. (2023). Match-based solution of general parametric eigenvalue problems. arXiv preprint arXiv:2308.05335.
- [13] Kappesser, M., Ziegler, A., & Schöps, S. (2024). Reduced Basis Approximation for Maxwell's Eigenvalue Problem and Parameter-Dependent Domains. IEEE Transactions on Magnetics.
- [14] Gavryliuk, N. (2019). Approximations for parameter-dependent eigenvalue problems arising in structural vibrations (Doctoral dissertation, University of Southampton).

## **COPYRIGHT STATEMENT**

The authors confirm that they, and/or their company or organisation, hold copyright on all of the original material included in this paper. The authors also confirm that they have obtained permission from the copyright holder of any third-party material included in this paper to publish it as part of their paper. The authors confirm that they give permission, or have obtained permission from the copyright holder of this paper, for the publication and public distribution of this paper as part of the IFASD 2024 proceedings or as individual off-prints from the proceedings.